

# RSC Advances



This is an *Accepted Manuscript*, which has been through the Royal Society of Chemistry peer review process and has been accepted for publication.

*Accepted Manuscripts* are published online shortly after acceptance, before technical editing, formatting and proof reading. Using this free service, authors can make their results available to the community, in citable form, before we publish the edited article. This *Accepted Manuscript* will be replaced by the edited, formatted and paginated article as soon as this is available.

You can find more information about *Accepted Manuscripts* in the [Information for Authors](#).

Please note that technical editing may introduce minor changes to the text and/or graphics, which may alter content. The journal's standard [Terms & Conditions](#) and the [Ethical guidelines](#) still apply. In no event shall the Royal Society of Chemistry be held responsible for any errors or omissions in this *Accepted Manuscript* or any consequences arising from the use of any information it contains.

## Controllable synthesis of biosourced blue-green fluorescent carbon dots from camphor for the detection of heavy metal ions in water

Rohit Ranganathan Gaddam,<sup>a,b</sup> D Vasudevan,<sup>c</sup> Ramanuj Narayan,<sup>a</sup> and KVS N Raju\*<sup>a</sup>

<sup>a</sup> Polymers and Functional Materials Division, Indian Institute of Chemical Technology, Tarnaka 500007, Andhra Pradesh.

<sup>b</sup> Amity Institute of Nanotechnology, Amity University, Noida 201301, Uttar Pradesh, India.

<sup>c</sup> Electrodeics and electrocatalysis division, Central Electrochemical Research Institute, Karaikudi-630006, Tamil Nadu.

\*Corresponding author. Tel./fax: +91 40 27193991

E-mail address : kvsnrju@iict.res.in (or) drkvsnrju@gmail.com

---

### Abstract

We report a robust method for the synthesis of fluorescent Carbon dots (C dots) from camphor, providing an insight into the mechanism of C dot formation. Camphor is a biosourced hydrocarbon, which contains hexagonal ring in an open book fashion. Burning of camphor leads to the formation of soot comprising graphitic domains. The soot when treated with piranha solution disintegrates into smaller domains leading to the formation of C dots with size distribution  $\sim 1-4$  nm. The obtained C dots were carboxyl terminated which was confirmed from the infrared spectroscopic measurements. The D and G bands at  $\sim 1314$   $\text{cm}^{-1}$  and  $\sim 1586$   $\text{cm}^{-1}$  respectively in Raman Spectroscopy and peaks at  $25.01^\circ$  in X-ray Diffraction of C dots confirm the presence of graphitic domains. Photoluminescence studies were carried out which reveal exceptional fluorescence in the as prepared C dots. Interestingly the quantum yield is found to be around 21.16%, which is significantly higher than the values observed in previous reports. The current study deals with sensing of metal ions. Heavy metal cations like  $\text{Cd}^{2+}$  and  $\text{Hg}^{2+}$  were used to check whether they affect the fluorescence properties of C dots. Also other cations like  $\text{Zn}^{2+}$ ,  $\text{Fe}^{2+}$ ,  $\text{Cu}^{2+}$  also quenched fluorescence but with a different profile.

## 1. Introduction

Carbon is amongst the most interesting material owing to its diverse chemical nature which makes it the most targeted material for industrial applications.<sup>1</sup> Many of the carbon nanomaterials like nanotubes, nanofibers, nanorods, graphene etc. are widely researched and well established.<sup>2</sup> Recently, Carbon dots (C dots) have attracted tremendous attraction due to their unique physico-chemical properties. Until recently, carbon based materials were expected to be black in colour, with lower solubility in water and weak or no fluorescence. However C dots are highly fluorescent, water-soluble and less than 10 nm in size.<sup>3</sup> They also possess exceptional properties like high optical absorptivity, chemical stability, low toxicity and biocompatibility.<sup>4</sup> As a result they find potential applications in multiple fields like medical diagnosis,<sup>4</sup> bio imaging,<sup>5</sup> sensing<sup>6</sup> and photovoltaics.<sup>7, 8</sup> Several top down approaches like laser ablation,<sup>9</sup> arc discharge<sup>2</sup> and plasma treatment<sup>10</sup> have been employed for the synthesis of C dots. Most of these methods involve the use of toxic precursors and high-end equipment, which are not cost-effective. In order to overcome these drawbacks, certain bottom up approaches has been employed for the synthesis of C dots. These involve carbonization of sugars, glycerol etc. Even in these cases, the method needs to employ several stages of reaction, strong acids and other agents so as to improve the solubility and fluorescence of the so obtained C dots. These methods are also costly and time consuming.<sup>11</sup> As an advancement to the C dot synthesis, single step preparation methods for C dots were established that involve hydrothermal carbonization of chitosan, microwave synthesis and solution chemistry. However even these methods suffer from drawbacks pertaining to time consumption, stringent synthetic conditions and high cost. Keeping the above drawbacks in mind C dots has been recently synthesized by using eco-friendly bio-precursors like soya milk,<sup>12</sup> orange juice,<sup>13</sup> banana juice<sup>14</sup> etc. Even here, the size of C dots obtained is not as uniform as expected.

In the present work, we report the synthesis of water-soluble fluorescent C dots from biological sourced hydrocarbon. Here we use camphor ( $C_{10}H_{16}O$ ) as a precursor material for the synthesis of C dots. Camphor is natural hydrocarbon obtained from the tree *Cinnamomum camphora*. It is waxy, flammable, crystalline substance, which is white in colour, and volatile in nature.<sup>15</sup> It is a bicyclic saturated terpene, which exists in the optically active dextro and levo forms and also as a racemic mixture of

the two forms. Dextro-form is amongst the most naturally occurring form that occurs in the woods and leaves of camphor tree. The soot obtained from the incineration of camphor is non-toxic and also has been used in India for centuries in facial decoration purposes. Camphor has been used in the preparation of carbon nanotubes, graphene, carbon nano-onions, carbon nanoparticles etc. through chemical vapour deposition laser ablation and other methods.<sup>16-22</sup> To our best knowledge there is no report on the synthesis of C dot from camphor soot. The main reason to use camphor as a starting material is because of its biological origin, which is renewable in nature. Also camphor is comparatively cheaper and easily available source for synthesis of C dots. Therefore it is possible to synthesize C dots in bulk quantities.

For the synthesis of C dot (Fig. 1), camphor was initially subjected to incineration followed by collection of soot on a polished copper surface. The camphor soot was subjected to treatment with piranha solution, which was then filtered out. The obtained filtrate was bright yellow in colour under normal light with a bluish-green in colour when placed under UV light. The obtained C dots were then neutralized with sodium hydroxide and then subjected to dialysis. The obtained C dots were in the size range of 1-4 nm and also stable in water. The C dot solution was then used for the detection of heavy metal cations like mercury and cadmium along with other cations like ferrous, zinc and cupric in water by measuring change in the fluorescence.

## 2. Experimental

### 2.1 Materials

Camphor was obtained from the local market. Conc. Sulphuric acid, 30% hydrogen peroxide solution, Mercuric chloride and Cadmium Chloride, Ferrous sulphate, Zinc Sulphate and Cupric Chloride were purchased from SD Fine chemicals, Mumbai. All the chemicals were used as received without any further purification.

### 2.2 Synthesis of C dots

Five grams of camphor was taken in a copper crucible and subjected to combustion. The obtained 300 mg soot was collected on a polished copper plate. The soot was then treated with piranha solution ( $\text{H}_2\text{SO}_4$ :  $\text{H}_2\text{O}_2$  = 7:3) for 15 hours. Following this, the piranha solution was diluted with water and filtered out. The back 200 mg soot remained in the filter paper and the residue C dot was obtained in the piranha solution. The piranha solution was then neutralized with sodium hydroxide, which

leads to salt formation. Dialysis was then performed to obtain pure C dot in water. The dialysis tubing cellulose membrane was used in this dialysis process. The outside and inside of the dialysis tubing was rinsed with 20ml of DI water for 15 to 30 minutes to remove sodium azide preservative. The water was poured out and the step repeated with another 20ml of deionized water. The dialysis was done in three days by immersing the dialysis tube containing sample in deionized water. The deionised water was changed in every 2 hours. The sample solution inside the tubing contained the pure C dot that was used for further characterization.

### 2.3 Preparation of salt solutions

AR samples of Mercuric Chloride, Cupric Chloride, Ferric Sulphate, Zinc Sulphate and cadmium chloride were used for studies on fluorescence quenching of C dots upon addition of these metal ions. A 0.1 M stock solution of each of these substrates was prepared. 2 ml solution of C dot was taken in the cuvette for fluorescence measurement. To this, increasing amounts of ions (0.5, 1, 1.5  $\mu\text{M}$  and so on) were added as the case may be. With each addition, the solution was stirred and the fluorescence measured.

### 2.4 Instruments

Fourier Transform Infrared (FTIR) spectroscopy of synthesized samples was recorded by Thermo Nicolet Nexus 670 spectrometer. Raman spectra were recorded using Horiba JobinYvon Raman spectrometer with a laser excitation wavelength of 632.81nm. Transmission electron micrographs (TEM) were recorded on a JEOL JEM-100CX electron microscope for examining the carbon nanoparticles. X-ray Diffraction (XRD) patterns for camphor soot were obtained using a Siemens D-5000 X-ray diffractometer with Cu K $\alpha$  radiation of wavelength 1.54. The crystalline phase of C dot was investigated by an Expert Pro Phillips X-ray diffractometer. Fluorescence spectroscopy was performed with a Horiba Fluoromax 4 spectrophotometer at different excitation wavelengths. UV-vis absorption spectra were obtained using a Shimadzu 220V (E) UV-Vis spectrophotometer.

### 3. Results and Discussion

It is well known that camphor is a naturally occurring hydrocarbon that possesses ten atoms out of which seven are associated with the ring system and the rest are methyl carbons. Camphor has a hexagonal ring in an open book fashion as opposed to that of graphite. The burning of camphor could lead to formation of hexagonal and pentagonal radicals (Fig. 2). They combine together forming channel type of structure possessing graphitic domains leading to formation of camphoric soot.<sup>1,23</sup> The X-ray Diffraction (XRD) profile of camphor soot reveals the presence of graphitic domains. XRD peaks of the camphor soot possess two prominent peaks at 25.6° and 43.6° which can be attributed to the (002) and (100) plane of hexagonal graphite (Fig. S1). The Raman profile of camphor soot (Fig. S2) reveals the presence of D band and G band around 1330 cm<sup>-1</sup> and 1586 cm<sup>-1</sup>, which also confirms the presence of graphitic domains. This soot when treated with piranha solution followed by filtration not only terminates the soot with a carboxyl group but also leaves behind C dots in the filtrate. The piranha solution contains a mixture of sulphuric acid and hydrogen peroxide, which react together to produce hydronium ions, bisulphate ions and atomic oxygen. This atomic oxygen allows the piranha solution to dissolve the elemental carbons. Generally camphor soot is difficult to attack chemically, because of their potential stability and sp<sup>2</sup> hybridized surface carbon atoms (Fig.S3). However the nascent oxygen directly attaches on to the surface of camphor soot, forming a carbonyl group. The oxygen atom here deceptively takes an electron bonding pair from the central carbon and forming a carbonyl group, while simultaneously disrupting the bonds of the target carbon atom with one or more of its neighbours therefore catering the breakdown of soot into smaller carbon materials. This is a cascading effect where single atomic oxygen initiates disentanglement of the local bonding structure, which in turn allows the whole range of reaction to affect the carbon atoms finally leading to the formation of C dots.<sup>24, 25</sup> The XRD profile (Fig.S4) of C dot also reveals the pattern of disordered carbon at 25.01°, which is very close to the graphite (002) plane of hexagonal graphite.

The piranha solution treated C dots are acidic in nature, hence, it is necessary to neutralize the solution upto pH 7. For this reason sodium hydroxide was used which eventually lead to the formation of salt. Therefore dialysis was an important step to be performed to ensure the purity of C dots. The initially obtained C dots (before dialysis) were observed under TEM (Fig. 3a) which reveal that the majority of C dots

have size of ~1-4 nm (Fig. S5). Following the dialysis, the salt was removed and pure C dot of size ~4-8 nm (Fig. 3b) were obtained in water. The TEM images reveal that the C dots are finely dispersed and mostly spherical in nature with little or no agglomeration. However the increase in size of pure C dots is most likely due to the formation of hydrogen bonds between the carboxyl groups present on the surface of the C dot as revealed by the FTIR analysis. The FTIR spectra (Fig. 4a) also exhibit the C-O stretching frequency at around  $1124\text{ cm}^{-1}$ . The peak at  $1630\text{ cm}^{-1}$  could be attributed to stretching frequency C=O of aromatic carbonyl; the two peaks around  $1440$  and  $1560\text{ cm}^{-1}$  originate due to presence of aromatic C=C; the band at  $3000\text{--}3400\text{ cm}^{-1}$  is indicative of O-H and N-H stretching frequencies respectively. Prior to dialysis the C dots show similar peaks in the FTIR spectra (Fig. S6). However, there are certain differences to be noticed in the spectra of C dots before and after dialysis. It can be seen that the absorption spectra of  $\text{-C=O-}$  of pure C dot appears at a relatively low frequency of  $1630\text{ cm}^{-1}$  as compared to that of its non-dialysed counterpart ( $1635\text{ cm}^{-1}$ ). This indicates that 'red shift' of carboxyl group from  $1635$  to  $1630\text{ cm}^{-1}$  that may result from intermolecular hydrogen bonding between C dots. The formation of hydrogen bonding will strengthen the interaction between C dots and therefore cater the increase in size of C dots.<sup>26</sup> Also, it is noticed that the peak ( $1630\text{ cm}^{-1}$ ) of pure C dot is widened with intensity increased in comparison with its counterpart. The C dots before dialysis (Fig. S6) shows a broad stretching band at  $3445\text{ cm}^{-1}$  and the absorption band, which peaks at  $1635\text{ cm}^{-1}$  correspond to -OH stretching frequency. The absorption band of -OH moves from  $3445$  to  $3400\text{ cm}^{-1}$  in case of pure C dots. Also in Fig.S6 the strong and broad peak centred at  $1124\text{ cm}^{-1}$  and the small shoulder at  $994\text{ cm}^{-1}$  could be assigned to vibrational stretching frequencies of sulphate respectively. The strong and broad absorption band centred at  $618\text{ cm}^{-1}$  probably resulted from the combined absorptions of sulphate, the Na-O stretching vibrations and the Na-OH wagging vibrational mode of molecular water. Therefore, this reveals the presence of Sodium sulphate in carbon dots before dialysis. Pure carbon dots and also the camphor soot cease to have such sulphate absorption peaks in their respective FTIR spectra.

Raman spectra of graphitic carbon generally consist of two prominent bands namely G-band (G for graphite) and D-band (D for Defect). D band arises at around  $1350\text{ cm}^{-1}$ , which correspond to  $A_{1g}$  symmetry of disordered graphite that also reveals the

presence of graphitic domains in carbon nanomaterial. G-band could be established at around  $1580\text{ cm}^{-1}$ . This band is accredited to a Zone center mode of  $E_{2g}$  symmetry of single crystal graphite. The Raman spectra of C dot clearly show the D-band near  $1314.63\text{ cm}^{-1}$  and G-band at  $1586.27\text{ cm}^{-1}$ , which reveal similarities with that of graphitic carbon. Also a downward shift in D and G band of C dot as compared to camphor soot is observable. The intensity ratio of D and G band ( $I_D / I_G$ ) provides an insight into the extent of disorder and the ratio of  $sp^3/sp^2$  carbon atoms. The  $I_D / I_G$  ratio of the as prepared C dot is 1.284 where as the  $I_D / I_G$  ratio of pristine Camphor soot is 0.95. The Fig. 4b shows a broad D-band, which implies presence of increased disorder and decreased domain size.<sup>27</sup> The recombination of bonds of camphor soot during C dot formation introduces smaller graphitic domain sizes, leading to size distributions with a variety of bonding structures. These distributions of cluster with different sizes introduce a superposition of different Raman modes, which result in a broader line-width in the case of C dots (Fig. 4b). The integrated intensity ratio between G-band and D-band is inversely proportional to the grain size of graphite. The average graphitic domain size calculated from the Raman spectra is  $45.4\text{ \AA}$  for Camphor soot and  $30.9\text{ \AA}$  for pure C dots. The results support broadening of D-band and shrinking of domain size as compared to the camphor soot.<sup>27,28</sup>

The absorption spectrum of C dot (Fig. 5a) shows an edge at around  $325\text{ nm}$  and a narrow peak around  $250\text{ nm}$  which could be associated with the  $\pi-\pi^*$  transition of nanocarbon.<sup>29</sup> The C dots were also subjected to different excitation wavelengths from  $320-600\text{ nm}$  (Fig. 5b). It is seen that with increase in excitation wavelength the fluorescence peak shifted to higher wavelengths. The C dot also shows a blue fluorescence when exposed to UV light. Interestingly quantum yield is found to be around  $21.16\%$ , which is significantly higher than the values reported earlier.<sup>12-14</sup> Therefore, the C dots pose a potential application in bio-labeling, sensing and optoelectronic devices. From the FTIR analysis it is clear that the C dots are terminated with a carboxyl group on the surface. Therefore it is expected that the fluorescence property change when they react with metal ions. Quenching of fluorescence may occur due to energy transfer, charge diversion or surface absorption. The quenching mechanisms could be either static quenching or dynamic quenching. Though the heavy metal salts could be detected by using atomic absorption or emission spectroscopy, Inductively coupled plasma mass spectroscopy and spectrophotometric

detection using organic dyes. Though these methods are highly precise the cost-effectiveness and easy handling is the major concern.

Therefore easy and cost effective approaches are required. Hence we here use C dots for the detection of heavy metal ions in aqueous media. Heavy metal cation like  $\text{Cd}^{2+}$  and  $\text{Hg}^{2+}$  were used to check if they affect the fluorescence properties of C dots. As shown in Fig. 3c the fluorescence of C dots is affected by the addition of mercury salt, where it is possible to observe a substantial quenching effect. Mercury (II) ion is amongst the most dangerous and omnipresent pollutants, which is a potential threat to environment and also human health. It is well established that  $\text{Hg}^{2+}$  could easily penetrate the skin, gastrointestinal tissues and respiratory organs, finally leading to a fatal damage of the central nervous system followed by mitosis impairment and DNA damage.<sup>30</sup> The fluorescence signal decreases upon addition of micro molar concentration of  $\text{Hg}^{2+}$  (Fig. 6a). In case of semiconducting quantum dots the quenching of fluorescence is attributed to the effective electron transfer process via non-radiative electron-hole recombination annihilation.<sup>31</sup> In case of C dots further enquiry is required in order to establish a firm theory on fluorescence quenching with heavy metal ion addition. The Stern Volmer plot of the  $\text{Hg}^{2+}$  sensing has been depicted in Fig.5d. It is interesting to note the non-linear nature of Stern Volmer plot over the concentration of  $\text{Hg}^{2+}$ . This phenomena means that charge transfer mechanism between  $\text{Hg}^{2+}$  and C dot may be due to non-dynamic (Static) mechanism. In a static quenching mechanism the quenching occurs as a result of a non-fluorescent complex formation between fluorophore and the quencher. However, this is just a preliminary information, further investigation might be required to confirm the mechanism of quenching.

The addition of  $\text{Cd}^{2+}$  also shows a substantial quenching effect but comparatively less than that of mercury (Fig. 6). Since these C dots are non-toxic and biologically inert they are a potential solution for in vitro measurements of the mercury uptake dynamics. However, for the in vivo analysis of metal ions further research is needed to establish the effect of biological molecules on the speciation of the metal ions (cysteine residuals, proteins that are water soluble, other anionic cellular components, etc.) and their interaction with C dots. Apart from heavy metal ions like  $\text{Cd}^{2+}$ , other ions like  $\text{Zn}^{2+}$ ,  $\text{Fe}^{2+}$  and  $\text{Cu}^{2+}$  were also used to quench fluorescence of C dot (Fig. 6). It is well observable from the graph that each ion shows a different profile of sensing. Fig. 7 shows the difference of fluorescence intensity ratio ( $F_0 / F$ ) of the C dot

solution in the absence and presence of various metal ions. Each ion is found to have a different  $F_0/F$  ratio as compared to the other.<sup>32</sup> It is seen that the sensing of heavy metal cation in the presence of other metal ions might not be much favorable owing to the sensing behavior of C dot with other metal ions. This limitation could be overcome if we could conjugate the C dot with other functional groups that are specific to target material of interest. We hope to carry out such investigation of sensing specific heavy metal ion in the near future.

#### 4. Conclusions

The present report focuses on the synthesis of C dots from camphor. Camphor being a green hydrocarbon and non-toxic adds up to the eco-friendly nature of C dots. Apart from this the camphor soot and the C dots possess graphitic carbon domains, which was very much evident from XRD and Raman analysis. C dots also have an exceptional photoluminescence property in the ultraviolet regime which is also evident from FTIR spectra that the C dots were carboxyl terminated. The Quantum yield of C dot was found to be around 21.16%. Therefore C dots were used as simple but effective sensor. Heavy metal cations like  $Cd^{2+}$  and  $Hg^{2+}$  were introduced and their complex interaction with carboxyl group catered fluorescence quenching, which could be used to test the ion concentration in various water bodies as the case may be. Also other cations like  $Zn^{2+}$ ,  $Fe^{2+}$  and  $Cu^{2+}$  were used for probing. Each cation showed a different profile of sensing in their fluorescence spectra. Though we can correlate this with specificity, the study is just preliminary. Further investigation into the method of fluorescence quenching, specificity in sensing by anchoring a moiety onto C dot etc. needs to be carried out in the near future. C dot could open up potential avenues for research as an effective nanoprobe.

#### Acknowledgements

The present research work was supported by CSIR, India under Intel-Coat Project (CSC-0114). The authors would like to extend their thanks to the Director, CSIR-IICT for permitting the work to be carried out.

#### Notes and References

1. R. R. Gaddam, S. Kantheti, N. R. Narayan and KVS N Raju. *RSC Adv.*, 2014, **4**, 23043-23049

2. S. Zhu, Q. Meng, L. Wang, J. Zhang, Y. Song, H. Jin and B. Yang, *Angewandte Chemie*, 2013, 125, 4045.
3. L. Cao, M. J. Mezziani, S. Sahu and Y. P. Sun, *Acc. Chem. Res.*, 2013, **46**, 171.
4. (a) L. Zhou, J. Liu, X. Zhang, R. Liu, H. Huang, Y. Liu & Z. Kang, *Nanoscale*, 2014, **6**, 5831-5837. (b) W. Shang, X. Zhang, M. Zhang, Z. Fan, Y. Sun, M. Han & L. Fan, *Nanoscale*, 2014, **6**, 5799-5806
5. B. Kong, A. Zhu, C. Ding, X. Zhao, B. Li and Y. Tian, *Adv. Mater.*, 2012, **24**, 5844.
6. Y. Fang, S. Guo, D. Li, C. Zhu, W. Ren, S. Dong and E. Wang, *ACS Nano*, 2012, **6**, 400.
7. S. N. Baker and G. A. Baker, *Angew. Chem.*, 2010, **122**, 6876.
8. V. Gupta, N. Chaudhary, R. Srivastava, G. D. Sharma, R. Bhardwaj and S. Chand, *J. Am. Chem. Soc.*, 2011, **133**, 9960.
9. X. Yan, X. Cui, B. Li and L.-S. Li, *Nano Lett.*, 2010, **10**, 1869.
10. Y. P. Sun, B. Zhou, Y. Lin, W. Wang, K. A. S. Fernando, P. Pathak, M. J. Mezziani, B. A. Harruff, X. Wang, H. F. Wang, P. J. G. Luo, H. Yang, M. E. Kose, B. L. Chen, L. M. Veca and S. Y. Xie, *J. Am. Chem. Soc.*, 2006, **128**, 7756
11. J. Wang, C.F. Wang and S. Chen, *Angew. Chem.*, 2012, **124**, 9431.
12. H. Li, Z. Kang, Y. Liu and S. T. Lee, *J. Mater. Chem.*, 2012, **22**, 24230.
13. C. Zhu, J. Zhai and S. Dong, *Chem. Commun.*, 2012, **48**, 9367.
14. S. Swagatika, B. Birendra, K.M. Tapas and M. Sasmita, *Chem. Commun.*, 2012, **48**, 8835.
15. B. De and N. Karak, *RSC Advances*, 2013, **3**, 8286.
16. P. Dubey, K. M. Tripathi and S.K. Sonkar, *RSC Advances*, 2014, **4**, 5838-5844.
17. J. Travas-Sejdic, N. Aydemir, B. Kannan, D. E. Williams and J. Malmström, *J. Mater. Chem. B*, 2014, **2**, 4593-4609
18. M. Kumar and Y. Ando, *Carbon*, 2005, **43**, 533-540.
19. M. Kumar and Y. Ando, *J. Phys.: Conf. Ser.*, 2007, **61**, 643.
20. P. R. Somani, S. P. Somani and M. Umeno, *Chem. Phys. Lett.*, 2006, **430**, 56-59.
21. L. F. Cui, L. Hu, J. W. Choi and Y. Cui, *ACS Nano*, 2010, **4**, 3671-3678.
22. R. J. Andrews, C. F. Smith and A. J. Alexander, *Carbon*, 2006, **44**, 341-347.
23. M. Kumar and Y. Ando, *Diamond and related materials*, 2003, **12**, 998-1002
24. K. Mukhopadhyaya, K.M. Krishna and M. Sharon. *Carbon*, 1996, **34**, 251-264. D. Diemente, *J. Chem. Educ.*, 1991, **68**, 568.

25. K. S. Koh, J. Chin, J. Chia and C.L. Chiang, *Micromachines*, 2012, **3**, 427.
26. W. Zhang, A. A. Dehghani-Saniij and R.S. Blackburn. *Progress in Natural Science*, 2008, **18**, 801-805.
27. G. X. Chen, M. H. Hong, T. C. Chong, H. I. Elim, G. H. Ma and W. Ji, *J. Applied Physics*, 2004, **95**, 1455.
28. D. S. Knight and W. B. White, *J. Mater. Res.*, 1989, **4**, 385–393.
29. D. Pan, J. Zhang, Z. Li, C. Wu, X. Yana and M. Wu, *Chem. Commun.*, 2010, **46**, 3681.
30. L. Zhou, Y. H. Lin, Z. Z. Huang, J. S. Ren and X. G. Qu, *Chem. Commun.*, 2012, **48**, 1147.
31. Y.S. Xia and C. Q. Zhu, *Talanta*, 2008, **75**, 215.
32. F. Wang, Z. Gu, W. Lei, W. Wang, X. Xia and Q.Hao - *Sensors and Actuators B: Chemical*, 2014, **190**, 516-522

## LIST OF FIGURES



**Fig. 1** Illustration of the formation of C dots from thermal dissociation of camphor

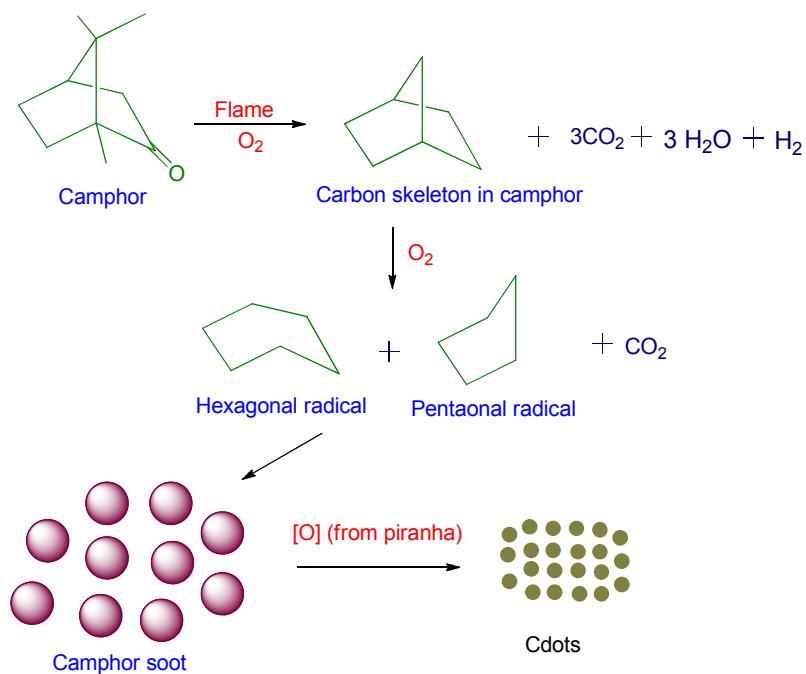


**Fig. 2** Possible mechanism for the formation of C dots from thermal dissociation of camphor

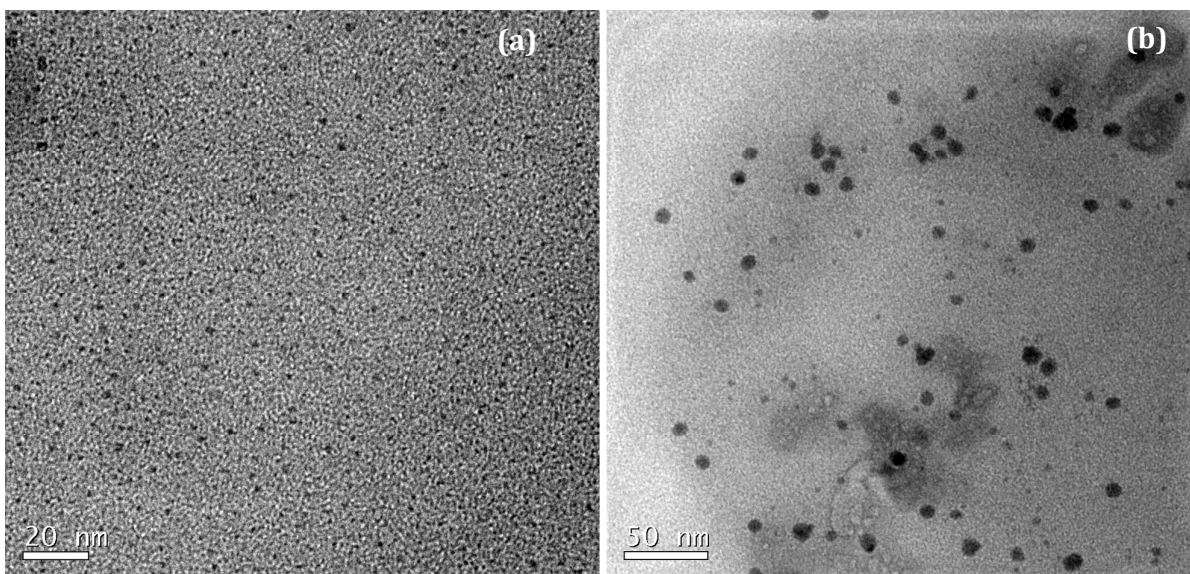


**Fig. 3** TEM images of (a) as prepared C dots (~1nm) with salt impurities, (b) C dots post dialysis.

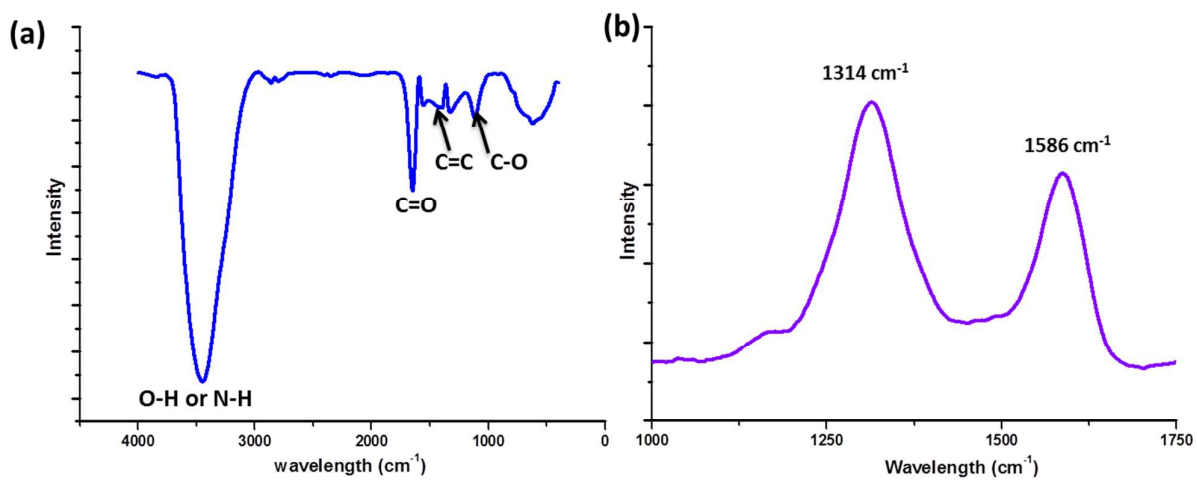


**Fig. 4** (a) FTIR spectra of C dot and (b) Raman spectra ( $\lambda_{\text{ex}} = 633\text{nm}$ ) of C dot

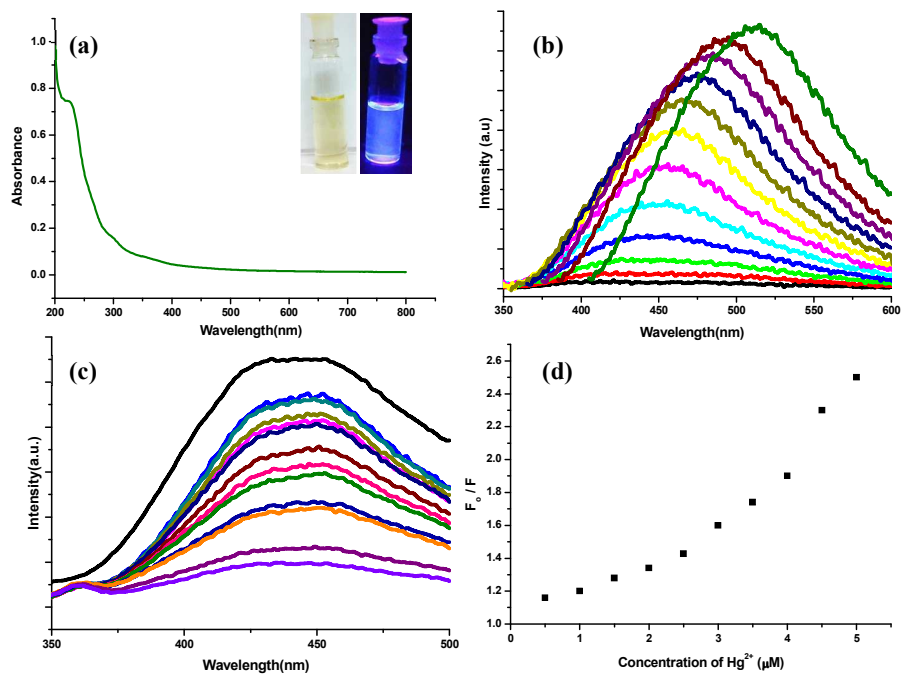


**Fig. 5** (a) Absorption spectra of C dot, inset: C dot showing a blue fluorescence when illuminated under UV lamp. (b) Photoluminescence spectra of C dot form 300 nm excitation with a 20nm increase in each step. (c) Fluorescence quenching by the addition of (0.5μl to 6μl) of mercury salt in an increasing order into 2ml of stock C dot solution ( $\lambda_{\text{ex}} = 320 \text{ nm}$ ) (d) Stern Volmer plot describing the dependency of fluorescence intensity on the concentration of  $\text{Hg}^{2+}$

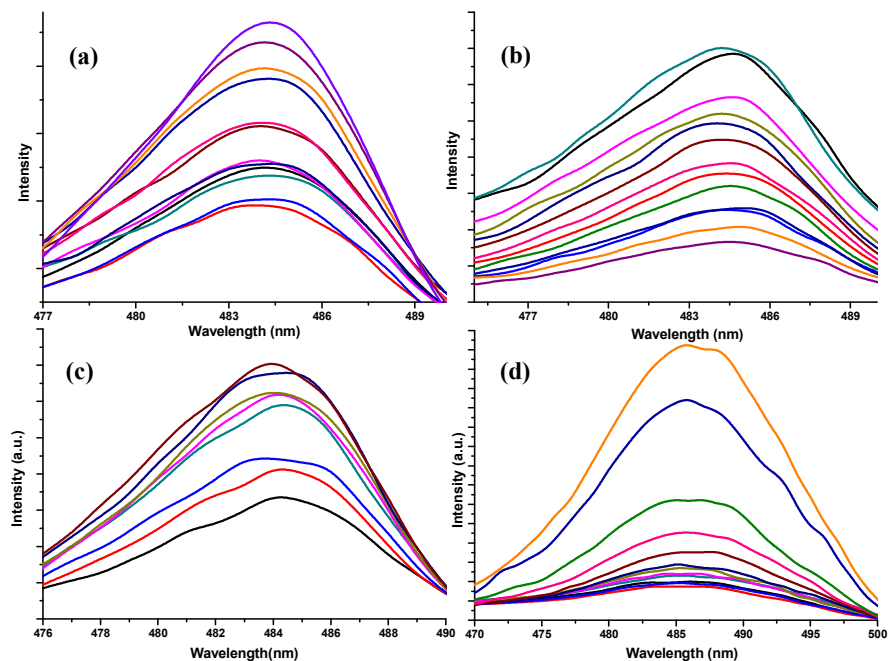


**Fig. 6** Fluorescence quenching by the addition of metal ions (0.5 $\mu$ l to 6 $\mu$ l of salt in an increasing order into 2ml of stock C dot solution) (a) Zn<sup>2+</sup>, (b) Cu<sup>2+</sup>, (b) Cd<sup>2+</sup> and (d) Fe<sup>2+</sup> (The excitation wavelength of  $\lambda_{ex} = 320$  nm was maintained)

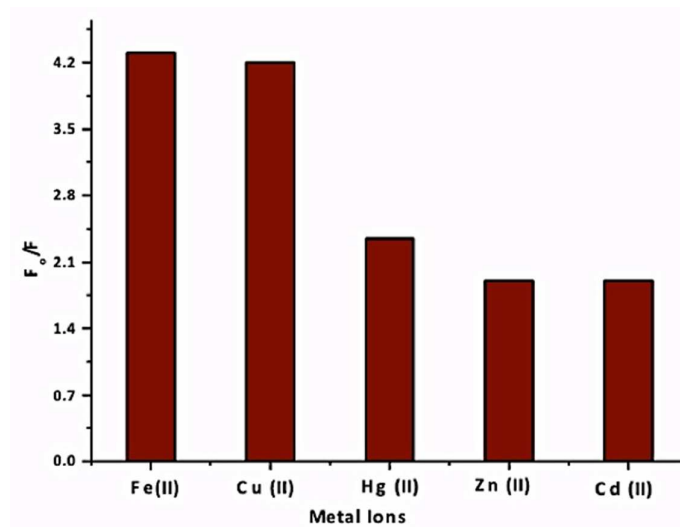


**Fig. 7** The graph represents various fluorescence intensity ratio ( $F_0/F$ ) of the C dot solution in the absence and presence of various individual metal ions.  $F_0$  and  $F$  are the fluorescence intensity at 320 nm in the absence and presence of ions, respectively.